A&A 521, A23 (2010)
DOI: 10.1051/0004-6361/201014884

Astronomy & Astrophysics

Impactor flux and cratering on the Pluto-Charon system

G. C. de Elía, R. P. Di Sisto, and A. Brunini

Facultad de Ciencias Astronómicas y Geofísicas, Universidad Nacional de La Plata and Instituto de Astrofísica de La Plata, CCT La Plata-CONICET-UNLP Paseo del Bosque S/N (1900), La Plata, Argentina
e-mail: gdeelia@fcaglp.unlp.edu.ar

Received 28 April 2010 / Accepted 2 July 2010

ABSTRACT

Aims. We study the impactor flux and cratering on Pluto and Charon caused by the collisional evolution of Plutinos. Plutinos are trans-Neptunian objects located at ~39.5 AU, in the 3:2 mean motion resonance with Neptune.
Methods. We develop a statistical code that includes catastrophic collisions and cratering events, and takes into account the stability and instability zones of the 3:2 mean motion resonance with Neptune. Our numerical algorithm proposes different initial populations that account for the uncertainty in the size distribution of Plutinos at small sizes.
Results. Depending on the initial population, our results indicate the following. The number of $D > 1$ km Plutinos streaking Pluto over 3.5 Gyr is between 1271 and 5552. For Charon, the number of $D > 1$ km Plutino impactors is between 354 and 1545. The number of $D > 1$ km craters on Pluto produced by Plutinos in the past 3.5 Gyr is between 43 076 and 113 879. For Charon, the number of $D > 1$ km craters is between 20 351 and 50 688. On the other hand, the largest Plutino impactor onto Pluto has a diameter of between ~17 and 23 km, which produces a crater with a diameter of ~31–39 km. In the same way, the largest Plutino impactor onto Charon has a diameter of between ~10 and 15 km, which produces a crater with a diameter of ~24–33 km. Finally, we test the dependence of results on the number of Pluto-sized objects in the Plutino population. If two Pluto-sized objects are assumed in the 3:2 Neptune resonance, the total number of Plutino impactors onto both Pluto and Charon with diameters $D > 1$ km is a factor of ~1.6–1.8 larger than that obtained considering only one Pluto-sized object in this resonant region.
Conclusions. Given the structure of the trans-Neptunian region, with its dynamically different populations, it is necessary to study in detail the contribution of all the potential sources of impactors onto the Pluto-Charon system, to determine the main contributor and the whole production of craters. Then, we will be able to contrast those studies with observations, which will help us to understand the geological processes and history of the surface of those worlds.

Key words. methods: numerical – Kuiper belt: general – planets and satellites: individual: Pluto

1. Introduction

Pluto and Charon are members of a vast population of icy bodies beyond Neptune and constitute the first discovered binary trans-Neptunian object (TNO). In the trans-Neptunian region, there are four dynamical classes (Chiang et al. 2007): the classical objects with semimajor axes a greater than ~42 AU and low eccentricity orbits, the scattered disk objects (SDOs) with perihelion distances of $q > 30$ AU and high eccentricities, the resonant objects in mean motion resonances with Neptune, and the centaurs with perihelion distances of $q < 30$ AU.

The 3:2 mean motion resonance with Neptune, located at ~39.5 AU, is the most densely populated one in the trans-Neptunian region. The residents of this resonant region are usually called Plutinos because of the analogy of their orbits with that of Pluto, which is its most representative member. Apart from Pluto and its largest moon Charon, the Minor Planet Center (MPC) database contains ~200 Plutino candidates.

Pluto and Charon have been exposed to impacts with minor bodies as all the objects in our Solar System. Cratering is one of the most important processes determining the morphology of the surface of a Solar System object. The understanding and quantification of the impactor source population onto an object and the observation of the object surface help us to understand the dynamical and physical history of both the impactor population and the target.

All of the detailed knowledge of the surface composition of Pluto and Charon has been obtained from telescopic observations of the spectrum of sunlight reflected from their surfaces. Pluto's reflectance spectrum shows absorption bands of methane ice, and an absorption band that could be related to the presence of CO and nitriles. The surface of Charon can be modeled by pure water ice darkened by a spectrally neutral continuum absorber (Protopapa et al. 2008).

However, it will not be until 2015 that we will have a real idea of the morphology of the surfaces of Pluto and Charon, with the fly-by of the Nasa's New Horizon Pluto-Kuiper belt mission to Pluto system. The New Horizons mission is the first one to the Pluto system and the Kuiper belt, and was launched on 19 January 2006 on a Jupiter Gravity Assist trajectory toward the Pluto system for a 14 July 2015 closest approach. It will study the Pluto system over a 5-month period beginning in early 2015 in particular providing measurements of cratering records.

The comparison of the predicted theoretical crater production from a given source with the observed surface of Pluto and Charon may account for the geological processes acting on the surface of the objects and if cratering collisions onto Pluto and Charon are an important surface modification process.

It is then very important to study all the possible sources of crater production on Pluto and Charon to characterize the total crater production and compare it with observations.

The possible main contributors to the impactor flux on Pluto and Charon would be on the one hand all type of comets. This topic has been addressed by Weissman & Stern (1994), Durda & Stern (2000), and Zahnle et al. (2003). In general, comets have eccentric orbits that can cross Pluto's orbit when they enter the planetary region from their source, either the trans-Neptunian zone or the Oort cloud, or when they leave the inner Solar System because of the perturbations of the planets.

Weissman & Stern (1994) estimated current impact rates of comets on Pluto and Charon. They showed that cratering on both bodies is dominated by Kuiper belt and inner Oort cloud comets. Durda & Stern (2000) then calculated collision rates in the Kuiper belt and Centaur region by means of a numerical model. They estimated that the flux of Kuiper belt projectiles onto Pluto and Charon is ~3–5 times that of Weissman & Stern (1994). Zahnle et al. (2003) studied the cratering rates for the moons of the jovian planets and Pluto produced mainly by ecliptic comets, obtaining results consistent with the previous estimates. We later analyze these studies in a discussion section.

On the other hand, Plutinos may be the other important source of impactors on Pluto and Charon. Plutinos shared the same dynamical conditions as Pluto and Charon, they are all located in the same 3:2 mean motion resonance with Neptune so they have a certain collision probability. de Elía et al. (2008) simulated the collisional evolution of Plutinos and determined collisional rates among these objects. This work allowed us to study the impactor flux on Pluto and Charon caused by the collisional evolution of Plutinos. In this paper, we evaluate the contribution of Plutinos to the impactor flux and cratering on Pluto and Charon and also determine whether the Plutino population can be considered a primary source of impactors on the Pluto-Charon system.

2. The full model

To simulate the collisional and dynamical evolution of the Plutino population, we use the statistical code developed by de Elía et al. (2008). This algorithm considers catastrophic collisions and cratering events, and takes into account the main dynamical characteristic associated with the 3:2 mean motion resonance with Neptune. In the following, we give a brief description of the initial populations, the collisional parameters and the main dynamical considerations used in our model.

2.1. Initial populations

From Kenyon et al. (2008), the cumulative size distribution of the resonant population of the trans-Neptunian region displays a break at a diameter D near 40–80 km. For larger resonant objects, the population seems to have a shallow size distribution with a cumulative power-law index of ~3. From this, the general form of the cumulative initial population used in our model to study the collisional and dynamical evolution of the Plutinos can be written as

$$N(>D) = C_1\left(\frac{1\ \mathrm{km}}{D}\right)^p \quad \text{for} \quad D \leq 60\ \mathrm{km},$$
$$N(>D) = C_2\left(\frac{1\ \mathrm{km}}{D}\right)^3 \quad \text{for} \quad D > 60\ \mathrm{km}, \qquad (1)$$

where C_2 adopts a value of 7.9×10^9 and $C_1 = C_2\,(60)^{p-3}$ by continuity for $D = 60$ km. The size distribution of Plutinos at small sizes is uncertain and one can find different proposed power-law indices in the literature. Following the analysis of de Elía et al. (2008), we then use in our model three different initial populations, which are defined as follows:

- initial population 1, with a cumulative power-law index p of 3.0 for $D \leq 60$ km;
- initial population 2, with a cumulative power-law index p of 2.7 for $D \leq 60$ km;
- initial population 3, with a cumulative power-law index p of 2.4 for $D \leq 60$ km.

2.2. Collisional parameters

We adopt constant values of the intrinsic collision probability $\langle Pi_c\rangle$ and the mean impact velocity $\langle V\rangle$ for Plutinos derived by Dell'Oro et al. (2001). Based on a sample of 46 Plutinos, these authors computed values of $\langle Pi_c\rangle$ and $\langle V\rangle$ of $4.44 \pm 0.04 \times 10^{-22}$ km^{-2} yr^{-1} and 1.44 ± 0.71 km s^{-1}, respectively.

As for the impact strength, O'Brien & Greenberg (2005) showed that the general shape of the final evolved asteroid population is determined primarily by the impact energy required for dispersal Q_D, but variations in the shattering impact specific energy Q_S and the inelasticity parameter f_{ke} can affect this final population even if Q_D is held the same. According to these arguments, we decide to choose a combination of the parameters Q_S and f_{ke} that yield the Q_D law from Benz & Asphaug (1999) for icy bodies at 3 km s^{-1}.

de Elía & Brunini (2007) analyzed the dependence of their numerical simulations on the shattering impact specific energy Q_S. According to this work, the smallest gaps between Q_S and Q_D curves lead to the smallest wave amplitudes in the size distribution of the final evolved population as well as to the highest ejection rates of collisional fragments. Moreover, that study also indicates that the formation of families is more effective for the simulations with a small gap between Q_S and Q_D laws. Following these arguments, we decide to use two Q_S laws, $Q_{S,1}$, and $Q_{S,2}$, with a small and a large gap with respect to the Q_D law from Benz & Asphaug (1999) for icy bodies at 3 km s^{-1}, respectively. The results discussed in this work are those obtained using the $Q_{S,1}$ law. In Sect. 3.4, we develop numerical simulations using the $Q_{S,2}$ law to test the dependence of our results on this collisional parameter. Figure 1 shows the two Q_S laws used in our simulations and the Q_D law from Benz & Asphaug (1999) for icy bodies at 3 km s^{-1}.

Once the Q_S law is specified, we fit the inelasticity parameter f_{ke} to obtain the Benz & Asphaug (1999) Q_D law. According to O'Brien & Greenberg (2005), we express the parameter f_{ke} as

$$f_{ke} = f_{ke_0}\left(\frac{D}{1000\ \mathrm{km}}\right)^\gamma, \qquad (2)$$

where f_{ke_0} is the value of f_{ke} at 1000 km and γ is a given exponent. Our simulations indicate that the Q_D law from Benz & Asphaug (1999) for icy bodies at 3 km s^{-1} is obtained with good accuracy from the combination of the selected Q_S law and f_{ke}, with $f_{ke_0} = 0.27$ and $\gamma = 0.7$. These values are consistent with those from Davis et al. (1989).

2.3. Dynamical considerations

To study the orbital space occupied by the Plutino population, we develop a numerical integration of 197 Plutino candidates extracted from the Minor Planet Center database with semimajor axes between 39 and 40 AU. These objects are assumed to be massless particles subject to the gravitational field of the Sun

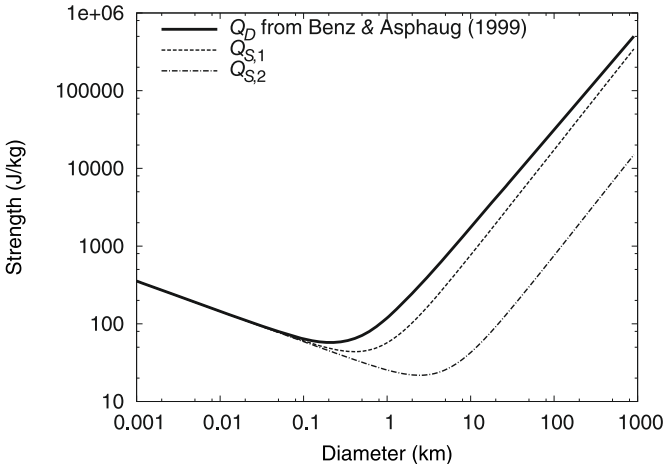

Fig. 1. Impact strength. The dashed lines represent the two different Q_S laws used in our simulations. The Q_D law from Benz & Asphaug (1999) for icy bodies at 3 km s^{-1} is plotted as a solid line.

(including the masses of the terrestrial planets) and the perturbations of the four giant planets. The simulation is performed with the simplectic code EVORB from Fernández et al. (2002). The evolution of the test particles is followed for 10^7 years, which is a timescale greater than any secular period found in this resonance (Morbidelli 1997). From this, we build maps of the distribution of Plutinos in the orbital element planes (a, e) and (a, i), which allows us to determine the main stability regions of the 3:2 Neptune resonance. These maps are used to assign a characteristic orbit for every colliding Plutino and to specify the final fates of the different fragments generated in the collisional evolution. A detailed description of this procedure can be found in de Elía et al. (2008).

3. Results

The previously described collisional code allows us to calculate the collisional rates of Plutinos onto Pluto and Charon. From this, it is possible to calculate the impactor flux of Plutinos of different sizes on the Pluto-Charon system. Using a suitable expression, we can calculate the crater diameters produced by Plutinos on Pluto and Charon. We present here our main results concerning the impactor flux and cratering onto Pluto and Charon due to the collisional evolution of the Plutino population.

3.1. Impactor flux onto Pluto and Charon

Figure 2 a) shows the cumulative number of Plutino impacts onto Pluto over the past 3.5 Gyr as a function of impactor diameter, obtained from the three different initial populations defined in Sect. 2.1. Moreover, Table 1 summarizes some of our results for the impactor flux onto Pluto produced by the collisional evolution of Plutinos. From this, the number of $D > 1$ km Plutinos striking Pluto over 3.5 Gyr is between 1271 and 5552, while the largest Plutino expected to have impacted Pluto during the past 3.5 Gyr had a diameter of ∼17–23 km, depending on the initial size distribution.

On the other hand, Fig. 2b) shows the cumulative number of Plutino impacts onto Charon over the past 3.5 Gyr as a function of impactor diameter. Moreover, results about the impactor flux onto Charon due to the collisional evolution of Plutinos are summarized in Table 2. From this, the number of $D > 1$ km Plutinos

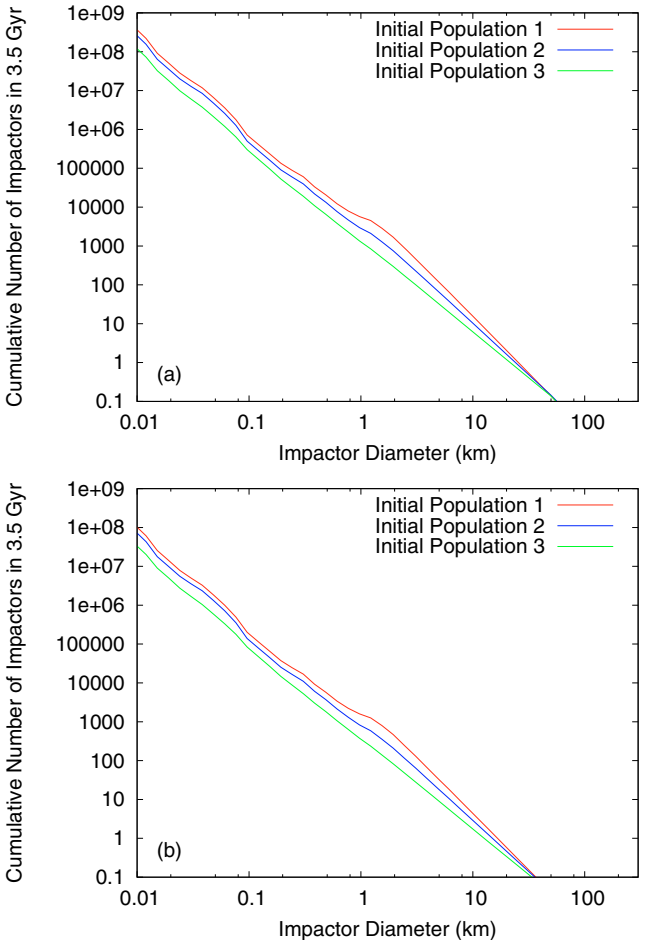

Fig. 2. Cumulative number of Plutino impactors onto Pluto **a)** and Charon **b)** over the past 3.5 Gyr as a function of impactor diameter.

Table 1. Collisional evolution results about Pluto.

	Initial Pop. 1	Initial Pop. 2	Initial Pop. 3
$N(D > 1)$	5552	2843	1271
$\tau(D > 1)$ (Myr)	0.63	1.23	2.75
$D_{\mathrm{i,Max}}$ (km)	22.5	20.1	16.8
$C(D > 1)$	113 879	76 726	43 076
$D_{\mathrm{c,Max}}$ (km)	38.8	35.5	30.1

Notes. $N(D > 1)$ is the total number of $D > 1$ km Plutinos impacting Pluto over 3.5 Gyr, $\tau(D > 1)$ the timescale on which these impacts occur, $D_{\mathrm{i,Max}}$ the largest Plutino expected to have struck Pluto during the past 3.5 Gyr, $C(D > 1)$ the total number of $D > 1$ km craters on Pluto produced by Plutino impacts over 3.5 Gyr, and $D_{\mathrm{c,Max}}$ the largest crater diameter on Pluto.

striking Charon over 3.5 Gyr is between 354 and 1545, while the largest Plutino expected to have impacted Charon during the past 3.5 Gyr had a diameter of ∼10–15 km, depending on the initial size distribution.

3.2. Cratering on Pluto and Charon

Using the impactor fluxes previously estimated, it is possible to calculate the number of craters on Pluto and Charon over the past

Table 2. Collisional evolution results about Charon.

	Initial Pop. 1	Initial Pop. 2	Initial Pop. 3
$N(D > 1)$	1545	791	354
$\tau(D > 1)$ (Myr)	2.27	4.42	9.9
$D_{\rm i,Max}$ (km)	14.6	12.5	9.8
$C(D > 1)$	50 688	34 541	20 351
$D_{\rm c,Max}$ (km)	32.7	28.9	24

Notes. $N(D > 1)$ is the total number of $D > 1$ km Plutinos impacting Charon over 3.5 Gyr, $\tau(D > 1)$ the timescale on which these impacts occur, $D_{\rm i,Max}$ the largest Plutino expected to have struck Charon during the past 3.5 Gyr, $C(D > 1)$ the total number of $D > 1$ km craters on Charon produced by Plutino impacts over 3.5 Gyr, and $D_{\rm c,Max}$ the largest crater diameter on Charon.

Table 3. Values of the density ρ, the surface gravity g, and the encounter velocity $v_{\rm i}$ used for Pluto and Charon.

	Pluto	Charon
ρ (g cm^{-3})	2.03	1.65
g (cm s^{-2})	66.4	27.9
$v_{\rm i}$ (km s^{-1})	1.9	1.6

3.5 Gyr as a function of crater diameter. From Holsapple (1993), the diameter $D_{\rm c}$ of a hemispherical crater is given by

$$D_{\rm c} = 1.26 D_{\rm i} (A\rho_{\rm i}/\rho_{\rm t})^{1/3} \left(1.61 g D_{\rm i}/v_{\rm i}^2\right)^{-\alpha/3}, \quad (3)$$

where $D_{\rm i}$ is the impactor diameter, $\rho_{\rm i}$ the impactor density, $\rho_{\rm t}$ the target density, g the surface gravity of the target, $v_{\rm i}$ the encounter velocity, and A and α are constants that depend on the mechanical properties of the target material. We adopt the values of $A = 0.2$ and $\alpha = 0.6$ given by Holsapple (1993) for water ice. The encounter velocity $v_{\rm i}$ is given by

$$v_{\rm i} = \left(U^2 + v_{\rm esc}^2\right)^{1/2}, \quad (4)$$

where U is the hyperbolic encounter velocity, which is equal to the mean impact velocity given in Sect. 2.2, and $v_{\rm esc}$ is the escape velocity of the target. Values of the density, the surface gravity, and the encounter velocity used for Pluto and Charon are shown in Table 3.

Figure 3 a) shows the cumulative number of craters on Pluto produced by Plutinos over 3.5 Gyr as a function of crater diameter. From this, the number of $D > 1$ km craters on Pluto is between 43 076 and 113 879, while the largest crater diameter is between ~31 and 39 km, depending on the initial size distribution.

In the same way, Fig. 3 b) shows the cumulative number of craters on Charon produced by Plutinos over 3.5 Gyr as a function of crater diameter. From this, the number of $D > 1$ km craters on Charon is between 20 351 and 50 688, while the largest crater has a diameter of ~24–33 km, depending on the initial size distribution.

3.3. Dependence of results on the number of Pluto-sized objects

Kenyon et al. (2008) suggested that the resonant trans-Neptunian population contains ~0.01–0.05 $M_\oplus$ in objects with $D \gtrsim 20$–40 km. From these estimates, it is possible to infer the existence of five Pluto-sized objects in the whole resonant population. If these five Pluto-sized objects were all in the 3:2 Neptune resonance, we would have an upper limit for the large objects in this resonance. Brown (2008), based on the completeness of the current surveys, argued that two or three more large KBOs are likely awaiting discovery. Since the existence of five Pluto-sized objects in the 3:2 Neptune resonance would seem to be an overestimation, we assume an upper limit of two Pluto-sized objects in this resonant region to analyze the dependence of our simulations on the number of large objects in this resonance.

If two Pluto-sized objects are assumed in the 3:2 Neptune resonance, the total number of Plutino impactors onto both Pluto and Charon with diameters $D > 1$ km is a factor of ~1.6–1.8 larger than that obtained considering only one Pluto-sized object in this resonant region.

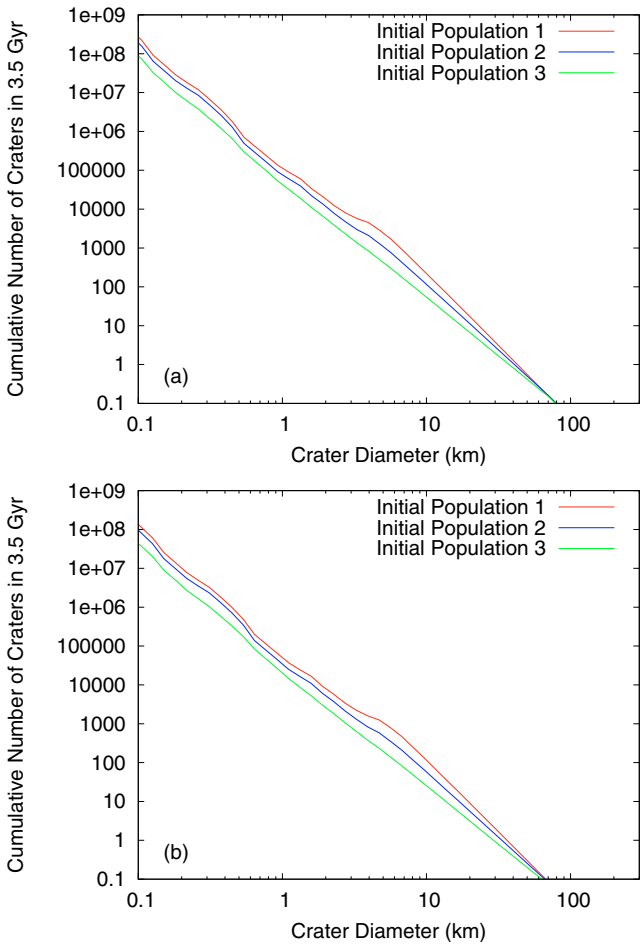

Fig. 3. Cumulative number of craters on Pluto a) and Charon b) produced by Plutinos over the past 3.5 Gyr as a function of crater diameter.

3.4. Dependence of results on the shattering impact specific energy Q_S

To test the dependence of our results on the shattering impact specific energy Q_S, we carry out numerical simulations using the $Q_{S,1}$ and $Q_{S,2}$ laws, which show a small and a large gap with respect to the Q_D law from Benz & Asphaug (1999) for icy bodies at 3 km s^{-1}, respectively. We find that the $Q_{S,2}$ law produces a size distribution with a wave amplitude larger than that of the one obtained using the $Q_{S,1}$ law as was noticed by de Elía & Brunini (2007). However, the whole impactor flux is almost preserved using both laws.

4. Discussion

Durda & Stern (2000) developed a model of collision rates in the present-day Kuiper belt and Centaur region consisting of a static, multizone, and multi-size-bin collision rate model that calculates instantaneous collision rates on Kuiper belt objects, Centaurs, and the Pluto-Charon system.

The model of Durda & Stern (2000) defines a disk in the 30–50 AU zone whose surface mass density follows a profile of the form $\Sigma \propto R^{-\beta}$, with $\beta = -2$. The disk adopts an average eccentricity $\langle e \rangle$ and assumes an equilibrium condition where the average inclination $\langle i \rangle = \frac{1}{2}\langle e \rangle$. The values adopted for $\langle e \rangle$ are 0.0256 and 0.2048, which are representative of the values observed in the Kuiper belt at that time. Once the disk properties are specified, the disk is binned into a series of radially concentric tori 1 AU in width in each of which the size distribution of the population is represented by a two-component power law of the form $N(D) \propto D^b \mathrm{d}D$, where $b = -3$ for $D < 10$ km and $b = -4.5$ for larger bodies. Durda & Stern (2000) carried out their runs assuming the existence of 7×10^4–1.4×10^5 objects with a radius $r > 50$ km between 30 and 50 AU, according to the observational evidence of Jewitt et al. (1998) and Gladman et al. (1998). Moreover, they suggested that about 40% of the total population are in or near the 3:2 mean motion resonance with Neptune. From this, the flux of $r = 1$ km Kuiper belt projectiles onto Pluto and Charon over 3.5 Gyr is found to be approximately 8.9×10^3 and 1.1×10^3, respectively.

However, the observational advances that have occurred in the past ten years have revealed a more complex dynamical structure of the trans-Neptunian region. In particular, in the region between 30 and 50 AU, there are very different dynamical classes of TNOs, such as the classical, resonant, and scattered-disk populations. They show different dynamical features and ranges of orbital elements as well-defined semimajor axis zones, eccentricities as high as ∼0.45 and inclinations as high as ∼45°. Moreover, current data provide clear evidence of differences in the mass and size distribution parameters among these dynamical classes (Kenyon et al. 2008). The results by Durda & Stern (2000) are obtained for objects in that region, but they do not account for the different dynamical populations. In particular, while the Plutino population is included quantitatively in Durda & Stern's (2000) model, they did not account for the dynamical properties of this resonant population. Their results should therefore be taken with caution.

5. Conclusions

We have presented an analysis of the collisional and dynamical evolution of the Plutinos. Assuming the existence of one Pluto-sized object in the 3:2 Neptune resonance, our main results are the following.

Our results depend strongly on the initial size distribution of Plutinos. Depending on the initial population, we have found that the number of $D > 1$ km Plutinos that have collided with Pluto in the past 3.5 Gyr is between 1271 and 5552. For Charon, the number of $D > 1$ km Plutino impactors is between 354 and 1545. Moreover, the number of $D > 1$ km craters on Pluto produced by Plutinos in the past 3.5 Gyr is between 43 076 and 113 879. For Charon, the number of $D > 1$ km craters is between 20 351 and 50 688. On the other hand, the largest Plutino impactor onto Pluto has a diameter of between ∼17 and 23 km, which produces a crater with a diameter of ∼31–39 km. The largest Plutino impactor onto Charon has a diameter of between ∼10 and 15 km, which produces a crater with a diameter of ∼24–33 km.

We have tested the dependence of our results on the number of Pluto-sized objects in the Plutino population. The number of Plutino impactors on Pluto and Charon obtained by considering two Pluto-sized objects is a factor of ∼1.6–1.8 larger than that obtained considering only one Pluto-sized object in this resonant region.

Using two different Q_S laws, with a small and a large gap with respect to the Q_D law, we have obtained almost the same impactor flux onto Pluto and Charon.

The complex structure of the trans-Neptunian region, with its dynamically different populations, requires a detailed study of the contribution of all the potential sources of impactor on the Pluto-Charon system, to obtain the main contributor and the whole production of craters. When Nasa's New Horizon Pluto-Kuiper belt mission flies by Pluto system, we will obtain images of the surface, and cratering records will be able to be measured. We will then be able to compare the theoretical studies of the production of craters with the observations of the New Horizon mission, which will help us to understand the geological processes and history of the surfaces of those worlds. In future work, we will calculate the contribution of the different dynamical classes of the trans-Neptunian region to the flux of projectiles onto Pluto and Charon. From this, it would be possible to specify the primary source of impactors on these bodies and to determine whether the Plutino population can be considered a significant source.

References

Benz, W., & Asphaug, E. 1999, Icarus, 142, 5

Brown, M. E. 2008, in The Solar System Beyond Neptune, ed. M. A. Barucci, H. Boehnhardt, D. P. Cruikshank, & A. Morbidelli (Tucson, USA: University of Arizona Press, 335

Chiang, E., Lithwick, Y., Murray-Clay, R., et al. 2007, in Protostars and Planets V, ed. B. Reipurth, D. Jewitt, & K. Keil (Tucson, USA: University of Arizona Press), 895

Davis, D. R., Weidenschilling, S. J., Farinella, P., Paolicchi, P., & Binzel, R. P. 1989, in Asteroids II, ed. R. P. Binzel, T. Gehrels, & M. S. Matthews (Tucson, USA: University of Arizona Press), 805

de Elía, G. C., & Brunini, A. 2007, A&A, 475, 375

de Elía, G. C., Brunini, A., & Di Sisto, R. P. 2008, A&A, 490, 835

Dell'Oro, A., Marzari, F., Paolicchi, P., & Vanzani, V. 2001, A&A, 366, 1053

Durda, D. D., & Stern, S. A. 2000, Icarus, 145, 220

Fernández, J. A., Gallardo, T., & Brunini, A. 2002, Icarus, 159, 358

Gladman, B., Kavelaars, J. J., Nicholson, P. D., Loredo, T. J., & Burns, J. A. 1998, AJ, 116, 2042

Holsapple, K. A. 1993, Annu. Rev. Earth Planet. Sci., 21, 333

Jewitt, D., Luu, J. X., & Trujillo, C. 1998, AJ, 115, 2125

Kenyon, S. J., Bromley, B. C., O'Brien, D. P., & Davis, D. R. 2008, in The Solar System Beyond Neptune, ed. M. A. Barucci, H. Boehnhardt, D. P. Cruikshank, & A. Morbidelli (Tucson, USA: University of Arizona Press), 293

Morbidelli, A. 1997, Icarus, 127, 1

O'Brien, D. P., & Greenberg, R. 2005, Icarus, 178, 179

Protopapa, S., Boehnhardt, H., Herbst, T. M., et al. 2008, A&A, 490, 365

Weissman, P. R., & Stern, S. A. 1994, Icarus, 111, 378

Zahnle, K., Schenk, P., Levison, H., & Dones, L. 2003, Icarus, 163, 263